EVALUATION OF THE VALIDITY OF THE TIBIA FRACTURE ASSESSMENT USING THE UPPER TIBIA ACCELERATION EMPLOYED IN THE TRL LEGFORM IMPACTOR

Atsuhiro Konosu [1], Takahiro Issiki [1], Yukou Takahashi [2]
[1] Japan Automobile Research Institute
[2] Japan Automobile Manufacturers Association, Inc.

ABSTRACT

The upper tibia acceleration of the TRL legform impactor has been used as an injury criterion of the tibia fracture to a pedestrian due to direct loading. In this research, its validity was evaluated by using two different analysis approaches. The results showed that the tibia acceleration of the TRL legform impactor has significantly low correlation with the bending moment exerted on a middle third of the human tibia. It was also found that the tibia acceleration poorly correlates with middle third tibia fractures observed in car-pedestrian accidents as a result of reanalysis of a past accident reconstruction study using the impactor.

Keywords: INJURY CRITERIA, INJURY PROBABILITY, IMPACTORS, PEDESTRIANS, LEGS

THE TRL LEGFORM IMPACTOR (TRL-LFI), which has rigid femur and tibia, has been used for the European directives (e.g. 2004/90/EC), the global technical regulations of the United Nation (gtr 9, 2009), and the New Car Assessment Program in Europe (Euro-NCAP). The TRL-LFI is instrumented with an accelerometer placed 66 mm below the knee joint to measure the upper tibia acceleration, and the acceleration is used for assessing a probability of tibia fracture of a pedestrian.

The evaluation method was introduced by the European Experimental Vehicles Committee Working Group 10 (EEVC/WG10) and the European Enhanced Vehicle-safety Committee Working Group 17 (EEVC/WG17) in 1994 and 1998, respectively, and the groups explained its validity in their working reports (EEVC, 1994 and EEVC, 1998). However, their explanations have not been fully clarified because some of the references were not made public but distributed as closed documents within the working group. This led to a large difficulty to evaluate the validity of the explanations especially for researchers who were not involved in the working group.

In 2003, one of those researchers tried to evaluate the validity of the tibia fracture evaluation method for the TRL-LFI by conducting accident reconstruction tests using the impactor (Matsui, 2003). In the research, based on the results of the accident reconstruction tests, it was concluded that the upper tibia acceleration of the TRL-LFI was a significantly meaningful measure (p value = 0.018) to evaluate tibia fractures to pedestrians which occur in actual traffic accidents. On the other hand, Bunketorp et al. (1981) conducted Post Mortem Human Surrogates (PMHS) tests, and found that the higher acceleration of legs were not well correlated with higher leg injury severities (p value > 0.5).

Several studies (Grosch, 1989, Kallieris, 1988, Otte, 2007) implied that there are two possible mechanisms of tibia fractures to pedestrians in car-pedestrian accidents. One mechanism (M1) of tibia fracture is direct loading (e.g. complex fracture) to the upper part of the tibia from the bumper of a car, resulting in local failure of the tibia near the point of application of the force. The other potential

mechanism (M2) of tibia fracture is due to bending of the tibia (e.g. oblique/wedge fracture) caused by inertial loading during car and pedestrian lower limb interaction. A simplified clarification on the fracture mechanism (M2) is given below with Figure 1 providing supplemental schematic:

Step 1: A car front has a clearance from the ground in general. During a car-pedestrian collision, a pedestrian foot and lower part of the leg (called as Distal Lower Limb (DLL) hereafter) are located in this space.

Step 2: When a car front impacts a pedestrian lower limb, the acceleration (a) is applied to the DLL in the coordinate system attached to the vehicle, and then the inertial force (F) obtained by multiplying the mass (m) by the acceleration of the DLL (a) is generated (F=ma).

Step 3: As a result, the bending moment (M) obtained by multiplying the inertial force (F) by the length from the center of gravity to the top of the DLL (L) is generated at the top of the DLL (M=FL).

Step 4: If the bending moment (M) exceeds the tibia tolerance in bending, the pedestrian lower limb would sustain fracture typically at the middle-third of the tibia, which interacts with the bumper and/or lower spoiler part of the car.

Interaction between an actual pedestrian lower limb and car front is much more complicated; however, the essence of the tibia fracture mechanism due to the inertia of the DLL can be explained as shown above.

Other potential mechanisms of fracture due to axial force or shear force would not be main factors/mechanisms for the following reasons. When we refer to the Tibia Index (Eppinger, 1999), the tibia tolerance in axial compression is 35.9 kN, which is an extremely high tolerance. Although the tibia tolerance in axial tension would be lower than that in compression, it would be in the same order of magnitude. Hayes and Gerhart (Bone and Mineral Research, 1985) shows that the ultimate strength of the femoral cortical bone in tension and compression are 133 and 193 MPa, respectively. Hayes and Gerhart also shows that the ratio of the ultimate strength of the femur in shear to that in compression is around 1.45. By applying the ratio to the tibia tolerance in compression, the tibia tolerance in shear is estimated as 24.8 kN, showing that the fracture tolerance of the tibia in shear is also very high. From the above analyses, tibia tolerance to the axial and shear loadings is extremely high, suggesting that axial or shear loading is unlikely to be a major factor for the tibia fracture of a pedestrian.

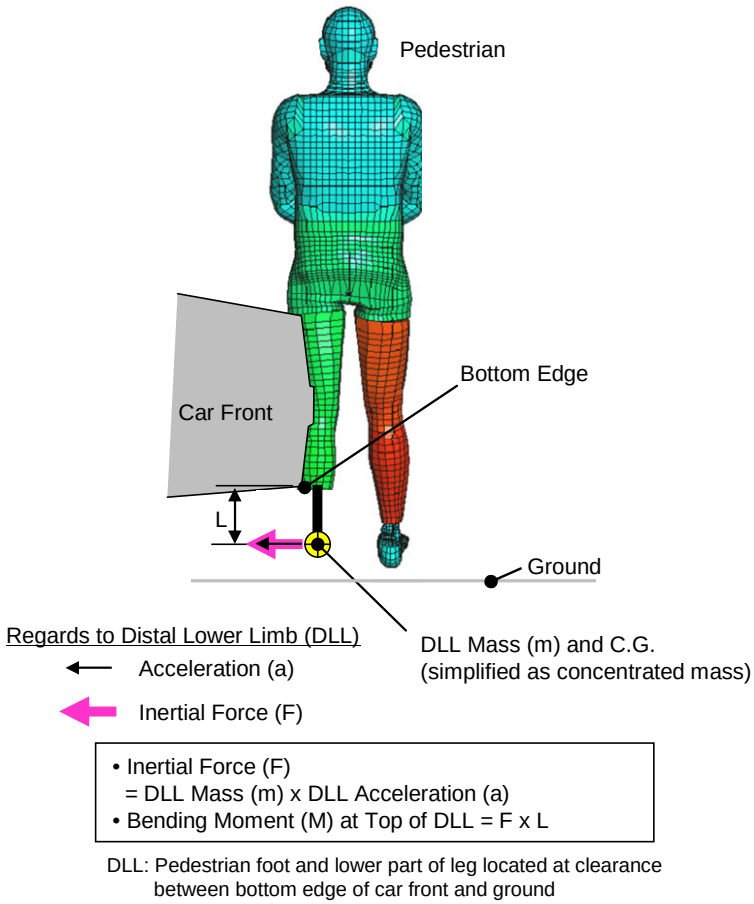

Fig. 1 – Tibia Fracture Mechanism by Inertia of Distal Lower Limb (Simplified Schematics)

Otte (2007) performed an accident analysis and found that leg fractures observed in pedestrian accidents were distributed in a wide range of the leg region (80% of all fractures were located between 19 cm and 46 cm from the ground level, i.e. middle third of the tibia shaft area), and detected that the percentage of leg fractures for which the height of the fracture site was identical to the bumper height was 17.5 % only. It means 82.5 % of the fractures occurred at the locations away from the bumper height level. The results led to a question on whether the upper tibia acceleration of the TRL-LFI can detect tibia fracture of a pedestrian thoroughly, although it is obvious that the upper tibia acceleration of the TRL-LFI well represent the direct loading mechanism (M1).

The current study focused on the evaluation of the validity of the tibia fracture assessment using the upper tibia acceleration of the TRL-LFI. This study was twofold; the first part of the study (A1) investigated the correlation between the upper tibia acceleration of the TRL-LFI and the tibia bending moment generated in the human tibia using a finite element (FE) model of the TRL-LFI and a human FE model. In order to investigate the correlation between the upper tibia acceleration of the TRL-LFI and tibia fractures sustained by pedestrians in car-pedestrian accidents, the second part of the study (A2) reanalyzed a past study by Matsui et al. (2003) that evaluated the validity of the tibia fracture evaluation method for the TRL-LFI by performing accident reconstruction tests using the impactor.

A1: ANALYSIS OF THE CORRELATION BETWEEN THE UPPER TIBIA ACCELERATION OF THE TRL LEGFORM IMPACTOR AND THE TIBIA BENDING MOMENT OF A HUMAN

In the first analysis (A1), the correlation between the upper tibia acceleration of the TRL-LFI and the bending moment of a human tibia was analyzed using the following computer simulation models; 1) TRL-LFI model, 2) Human model, and 3) Simplified car models.

TRL-LFI model: Figure 2 shows the TRL-LFI model. The model consists of the flesh part and body part. The flesh part was made by using deformable solid elements in order to simulate compression of the flesh during an impact with a car. The upper and lower parts of the body were modeled using rigid shell elements connected to each other using a kinematic joint model at the knee joint in order to simulate the shearing and bending motion of the knee.

Compression characteristics of the flesh part of the model were determined from compression tests of the material (Confor foam™) used for the flesh. Figure 3 shows the compression characteristics of the Confor foam™ obtained from the compression tests. The test conditions for the compression tests are illustrated in Figure 3. The Confor foam™ is highly sensitive to the temperature, therefore, the compression characteristics of the Confor foarm™ under 20 degrees Celsius, mean value of the temperature range allowed by EU Directives (e.g. 2004/90/EC) and gtr 9 (2009), was used in this analysis. This temperature is also the mean value of the tolerance of the temperature of the test site when the TRL-LFI is used.

The shearing and bending characteristics of the knee joint model are shown in Figure 4. Each of the characteristics fell within the shearing and bending requirement corridors of the TRL-LFI, almost exactly tracing the middle of the upper and lower bounds of the corridors.

The TRL-LFI model was validated at the assembly level under the dynamic certification test specified for the TRL-LFI (EEVC, 1998). The outputs with regard to the tibia upper acceleration, knee bending angle, and knee shearing displacement of the impactor model were comparable to the test results as shown in Figure 5. Each of the maximum values was within the TRL-LFI requirement corridors, and the waveforms were similar between the test and simulation results.

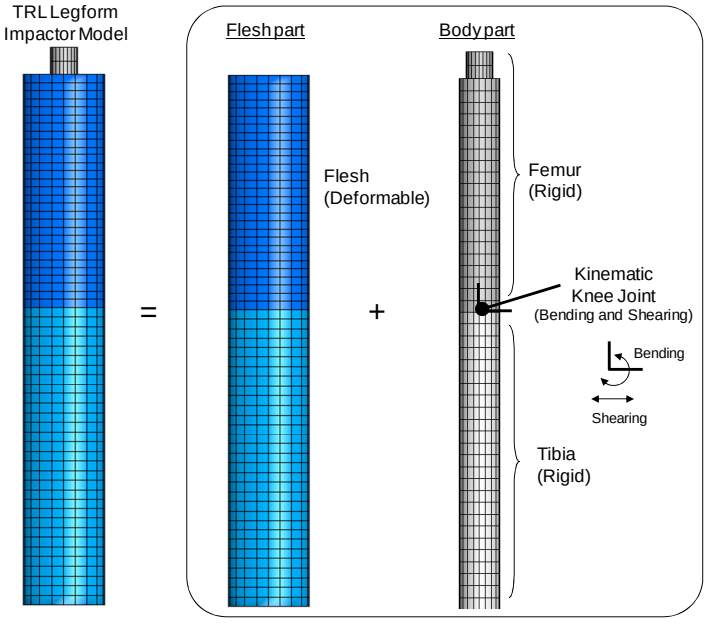

Fig. 2 - TRL Legform Impactor Model

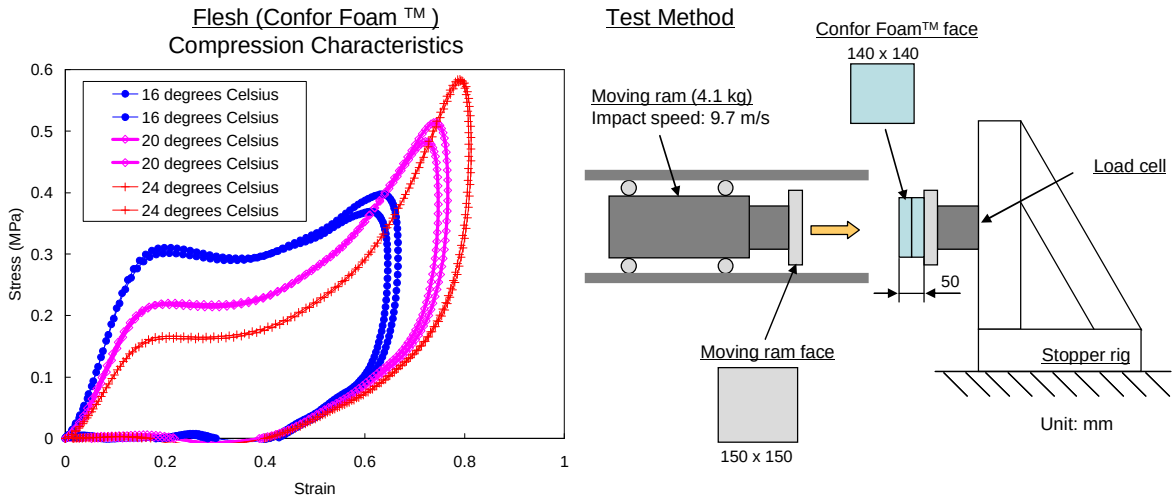

Fig. 3 - Compression Characteristics of Confor Foam ™

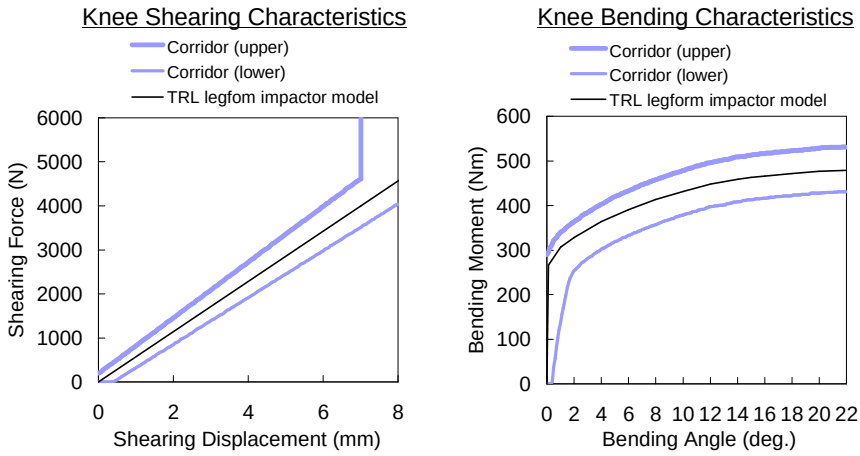

Fig. 4 - Knee Bending and Shearing Characteristics of TRL Legform Impactor Model

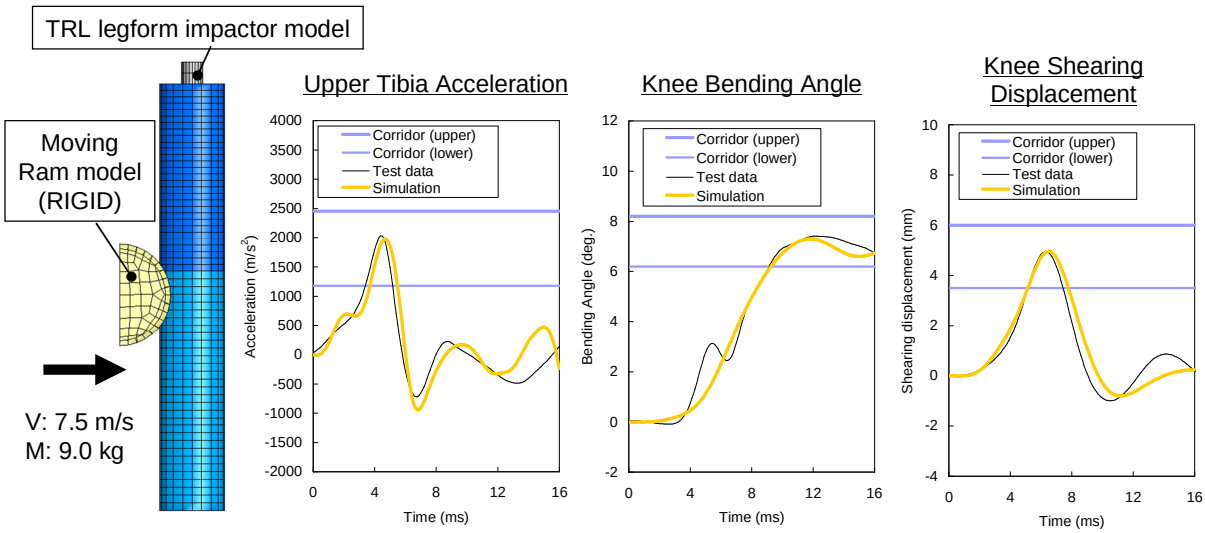

Fig. 5 - Dynamic Certification Test Simulation Results

Human Model: Figure 6 shows the human model used in this analysis. The model simulates a human body in detail by using finite element modeling technique, and the model was validated in a series of past studies (Takahashi et al., 2003, Kikuchi et al., 2006, Kikuchi et al., 2008). The model has been validated in terms of the following items, showing good correlation with the Post Mortem Human Subjects (PMHS) responses not only at the component levels but also at the assembly levels.

Validation items of the Human Model used in this study

Long Bones (Takahashi et al., 2003)
- Evaluation Parts: Femur, Tibia and Fibula
- Loading Configuration: Dynamic 3-point Bending
- Loading Locations: Proximal-Third, Mid-Shaft and Distal-Third

Long Bones with Flesh (Kikuchi et al., 2006)
- Evaluation Parts: Thigh
- Loading Configuration: Dynamic 3-point Bending
- Loading Locations: Mid-Shaft, Distal-Third

- Evaluation Parts: Leg
- Loading Configuration: Dynamic 3-point Bending
- Loading Locations: Proximal-Third, Mid-Shaft, Distal-Third

Knee Ligaments (Takahashi et al., 2003 and Kikuchi et al., 2006)
- Evaluation Parts: ACL, PCL, MCL and LCL
- Loading Configuration: Dynamic and Quasi-static Tension

Knee Joints (Takahashi et al., 2003 and Kikuchi et al., 2006)
- Evaluation Parts: Assembled
- Loading Configuration: Dynamic 4-point Bending

Lower Limb (Kikuchi et al., 2008)
- Evaluation Parts: Assembled
- Loading Configuration: Dynamic Full-Scale Car Impact

The model was also used in the evaluation study of the biofidelic Flexible Pedestrian Legform Impactor type GT (Konosu et al., 2007), and all of the settings of the human model were exactly the same as those of the study.

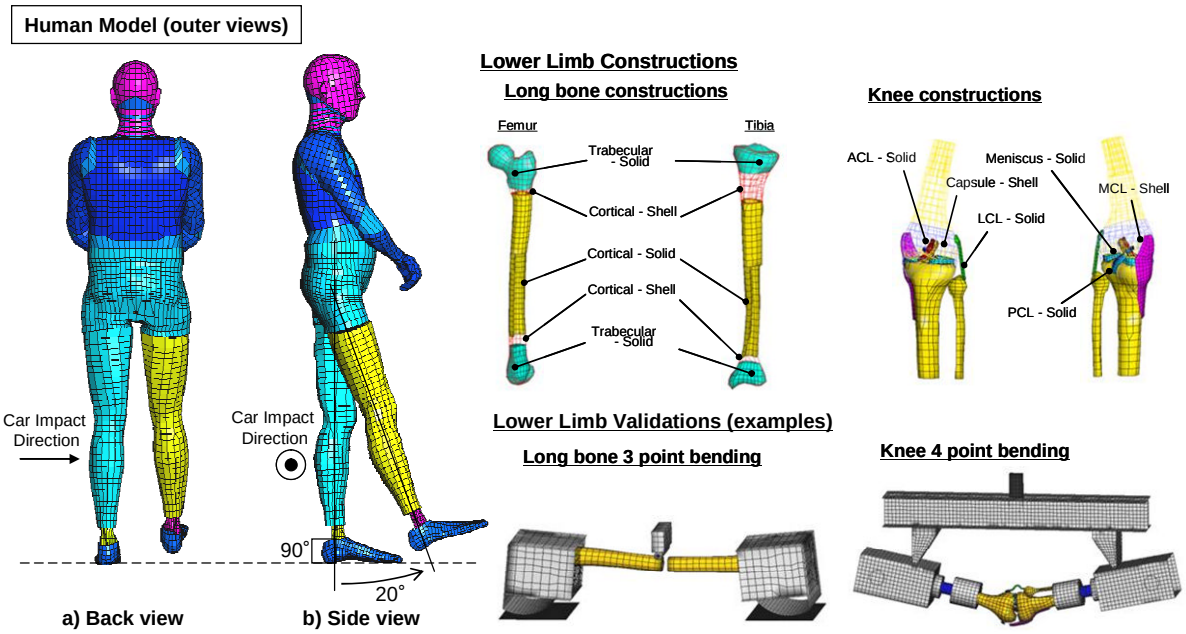

Fig. 6 - General Information for Human Model

Simplified Car Model: Figure 7 shows the structure of a simplified car model used in this analysis. The model consisted of 3 parts; bonnet leading edge (BLE), bumper (BP) and spoiler (SP). The BP and SP primarily generate the reaction force in longitudinal direction to the car. Therefore, simple 1-D joints were used for these components in order to obtain stable reaction force from the car during the impact simulation. On the other hand, the BLE was simulated by using deformable shell elements in order to represent realistic 3-D deformation around the BLE part of the car.

The stiffness of each of the parts can be changed by changing the thickness of the shell element (BLE) or changing the kinematic joint characteristics (BP and SP) as shown in Figure 8 through Figure 9. Figure 8 shows the force-displacement characteristics applied to the BP and SP kinematic joints used in this study. Figure 9 shows the examples of the force-deflection characteristics of the BLE for some different loading conditions. In this figure, the BLE was compressed by a 50 mm radius rigid ram with several different impact angles, which were selected based on possible pedestrian lower limb and simplified car impact situations.

In this analysis, 18 types (S1-S18) of simplified car models were used (see Table 1 and Figure 10) as well as the human model simulation results obtained from the evaluation study of the biofidelic Flexible Pedestrian Legform Impactor type GT (Konosu et al., 2007). All of the settings of the simplified car models were exactly the same as those used in the previous study.

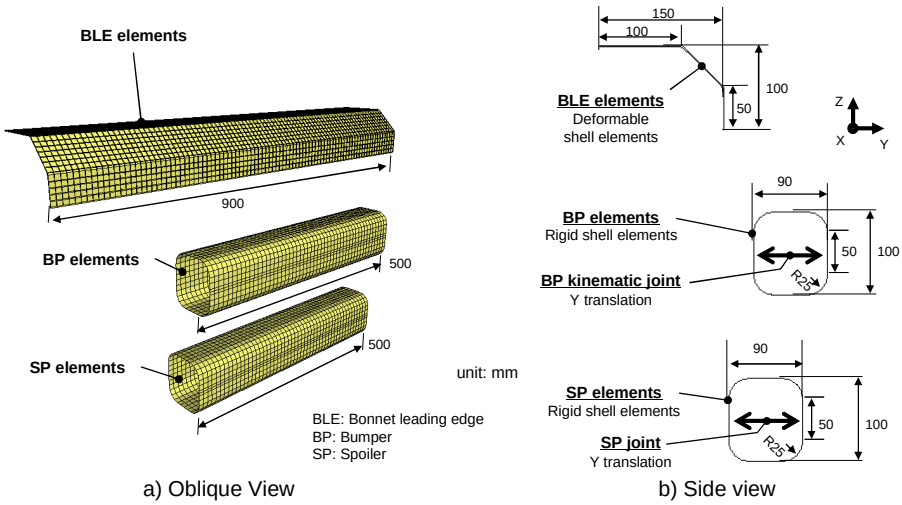

a) Oblique View b) Side view

Fig. 7 – Constructions for Simplified Car Model

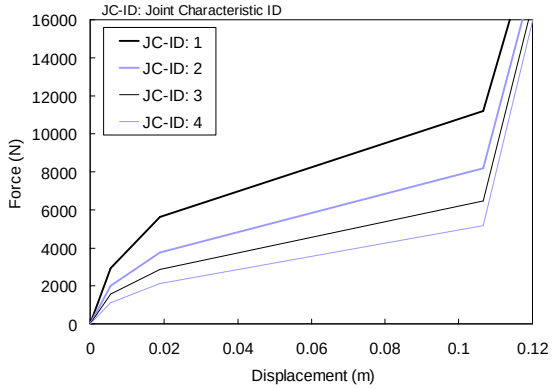

Fig. 8 – Joint Characteristics of BP and/or SP for Simplified Car Model used in this study

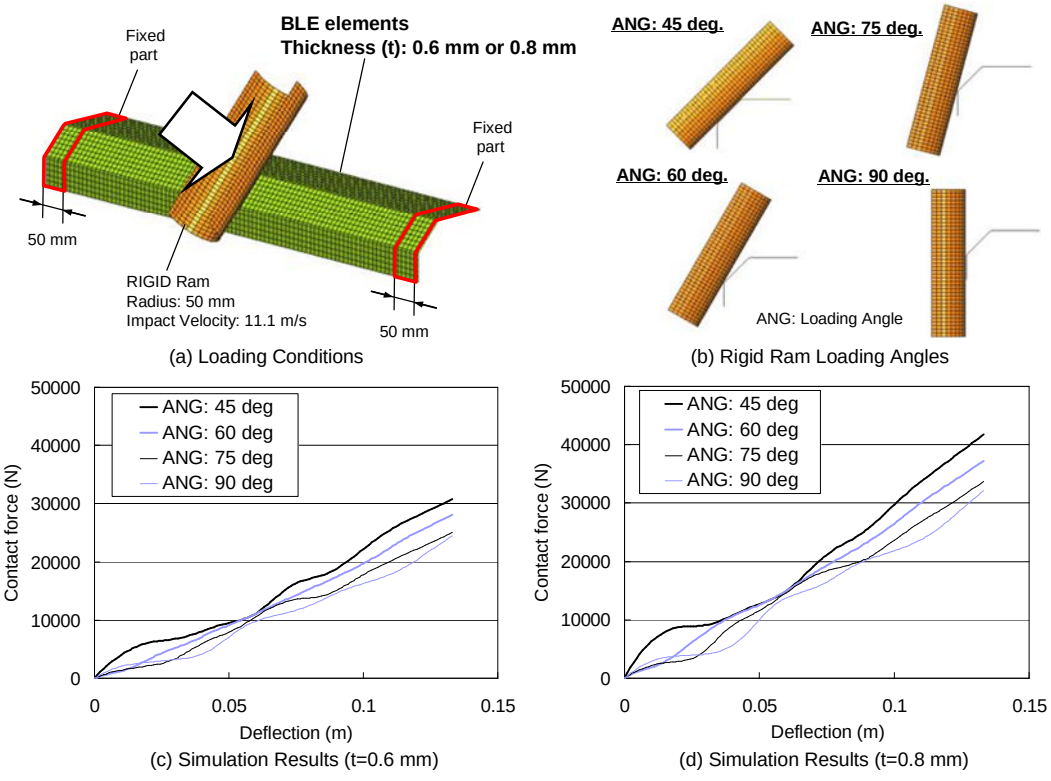

(a) Loading Conditions (b) Rigid Ram Loading Angles

(c) Simulation Results (t=0.6 mm) (d) Simulation Results (t=0.8 mm)

Fig. 9 – Deformation Characteristics of BLE for Simplified Car Model (examples)

Table 1: Specifications of 18 Simplified Car Models

Simplified Car model specifications

Simplified Car Model ID	K1 (BLE thickness*) mm	K2 (BP stiffness**) JC-ID	K3 (SP stiffness**) JC-ID	H1 (BLE height) mm	H2 (BP height) mm	H3 (SP height) mm	L1 (BLE lead) mm	L2 (SP lead) mm
S1	0.4	3	4	650	450	250	125	-20
S2	0.4	3	2	700	490	270	200	0
S3	0.4	3	1	750	530	350	275	30
S4	0.4	2	4	650	490	270	275	30
S5	0.4	2	2	700	530	350	125	-20
S6	0.4	2	1	750	450	250	200	0
S7	0.4	1	4	700	450	350	200	30
S8	0.4	1	2	750	490	250	275	-20
S9	0.4	1	1	650	530	270	125	0
S10	0.6	3	4	750	530	270	200	-20
S11	0.6	3	2	650	450	350	275	0
S12	0.6	3	1	700	490	250	125	30
S13	0.6	2	4	700	530	250	275	0
S14	0.6	2	2	750	450	270	125	30
S15	0.6	2	1	650	490	350	200	-20
S16	0.6	1	4	750	490	350	125	0
S17	0.6	1	2	650	530	250	200	30
S18	0.6	1	1	700	450	270	275	-20

BLE: Bonnet Leading Edge, BP: Bumper, SP: Spoiler, JC-ID: Joint Characteristics ID
* BLE stiffness was changed by changing steel plate thickness, ** BP and SP stiffness was changed by changing joint characteristics

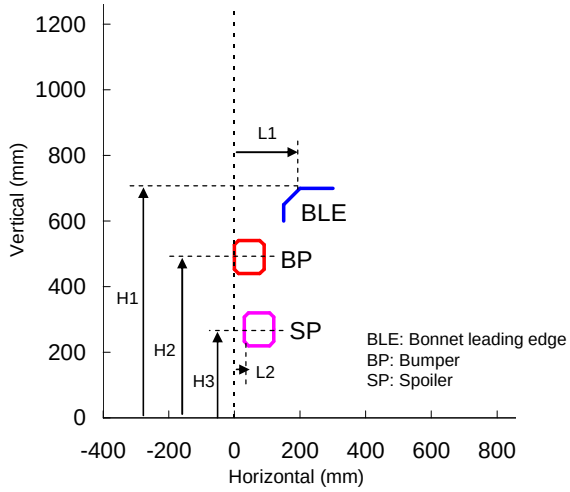

Fig. 10 - Definitions of Simplified Car Model Dimensions

METHODOLOGY: 18 types of simplified car models impacted the TRL-LFI model as well as the human model at the impact speed of 11.1 m/s. The impact height of the TRL-LFI and the human model was set at 25 mm above the ground level based on the gtr 9 (2009) impact condition, in which shoe sole height is considered (see Figure 11a). Impact condition of the simplified car model to the human lower limb (initial impact side) was the same as that of the TRL legform impactor. In other words, the human lower limb (initial impact side) was straight and vertical to the ground, and was impacted by the simplified car (see Figure 6 and Figure 11a). The human lower limb posture was set up based on the information obtained from a personal communication with an EEVC/TRL person, who knows well about the human lower limb setting simulated by the TRL legform impactor test.

In the computer simulation analysis, the upper tibia acceleration of the TRL-LFI model and the bending moment around the middle third of the tibia of the human model (see Figure 11b) were obtained, and then correlation between maximum values of these measures was analyzed.

Given that the bending moment is a primary factor of pedestrian tibia fractures, the use of the upper tibia acceleration of the TRL legform impactor as an injury criterion for human tibia fracture assumes a good quantitative correlation between the maximum upper tibia acceleration of the impactor

and the maximum bending moment of the human tibia. However, so far, this kind of quantitative correlation analysis has not been conducted yet. We therefore decided to quantitatively validate the correlation between them in the current study. The application of the element elimination option for simulating bone fractures introduces load-limiting events, and thus makes it unable to perform the quantitative correlation analysis described above. For this reason, in this research, it was decided not to apply the element elimination option to the human model for simulating bone fractures.

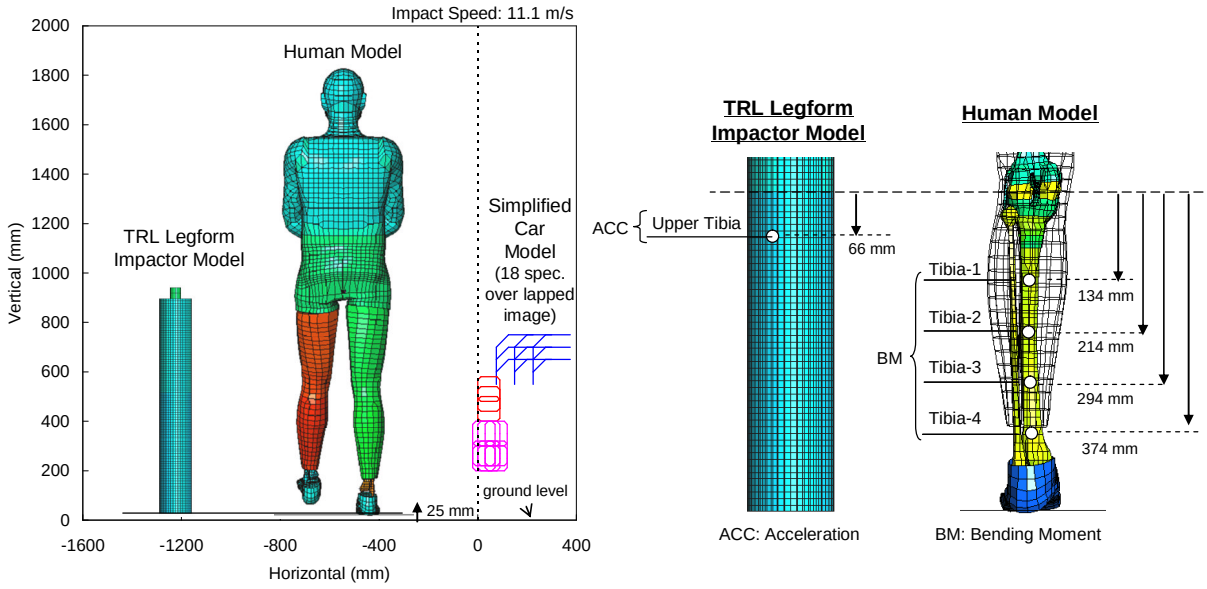

a) Impact Conditions b) Measurement Items

Fig. 11 – Impact Conditions (Image) and Measurement Items

RESULTS: Figure 12 shows the maximum values of the upper tibia acceleration of the TRL-LFI model and the bending moment for each tibia portion of the human model. The figure shows the tibia bending moment of the human model differs by the car type significantly. In many cases, the maximum tibia bending moment location was at Tibia-1 (proximal part of the Middle-Third-Shaft). This correlates with the fracture site distribution of the actual real-world accident cases (Otte et al., 2007). Besides, in nearly half of the cases (S2, S6, S8, S9, S10, S12 and S18), the maximum bending moment does not significantly differ between Tibia-1, Tibia-2 and Tibia-3. These cases imply that Tibia-2 and Tibia-3 (mid or distal part of the Middle-Third-Shaft) also have a chance to fracture in the real-world accidents.

Figure 13 shows the correlation between the maximum values of the upper tibia acceleration of the TRL-LFI model and the Tibia-All (all of the measured parts of the tibia) bending moment of the human model. The solid line represents the regression line obtained using a least square method. It is clear that the correlation is significantly low (R = 0.01). The regression line of the data is almost parallel to the horizontal axis. This result implies that the assessment of pedestrian tibia fractures due to bending using the upper tibia acceleration of the TRL-LFI is not adequate.

Figure 14 shows an example of two different simplified car models which generate comparable upper tibia acceleration of the TRL-LFI (S6: 1357 m/s^2, S16: 1371 ms/^{2}). Because of the difference in car front geometry, significantly different bending moments on the human tibia were observed (S6: 223 Nm, S16: 336 Nm).

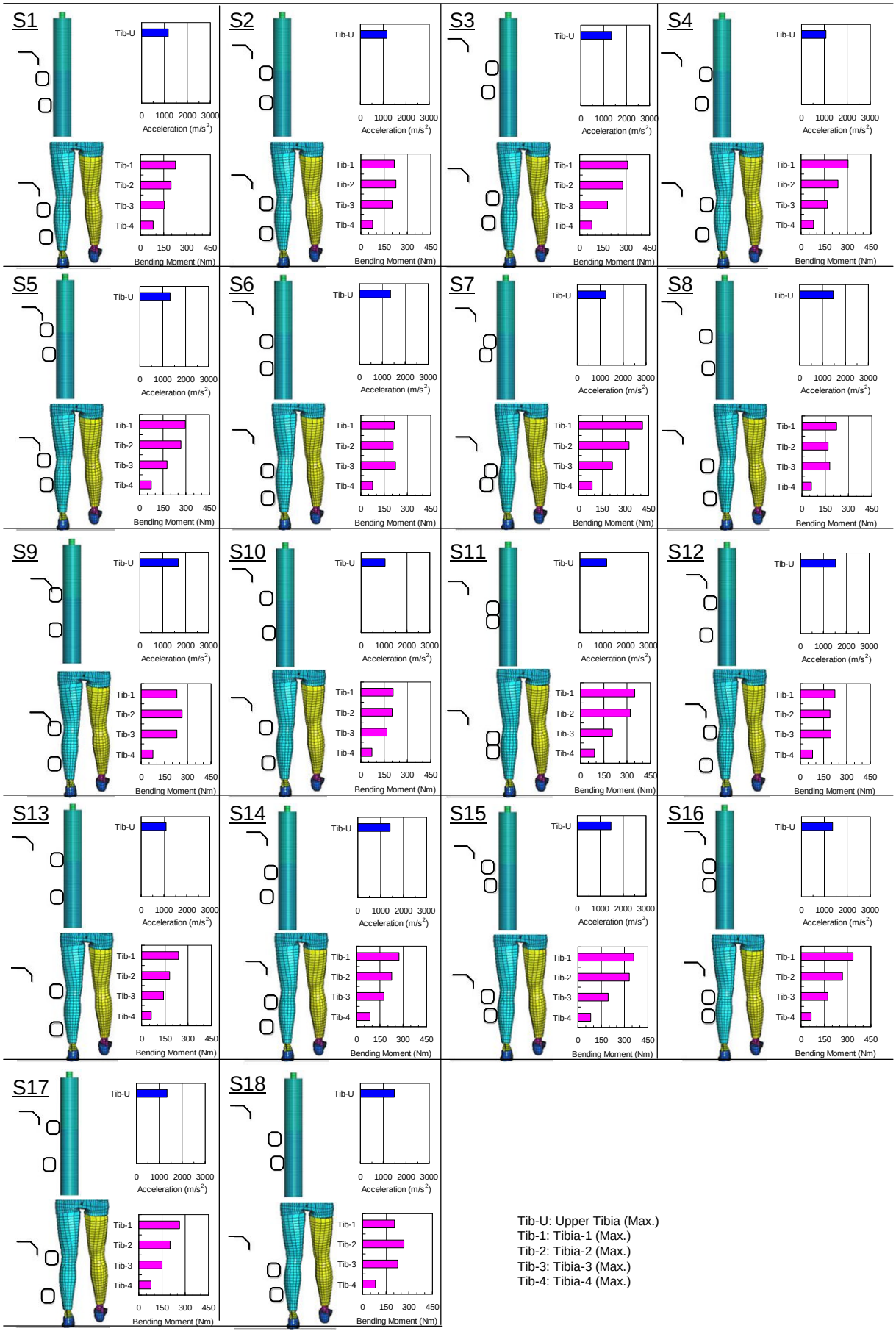

Fig. 12 – Computer Simulation Results

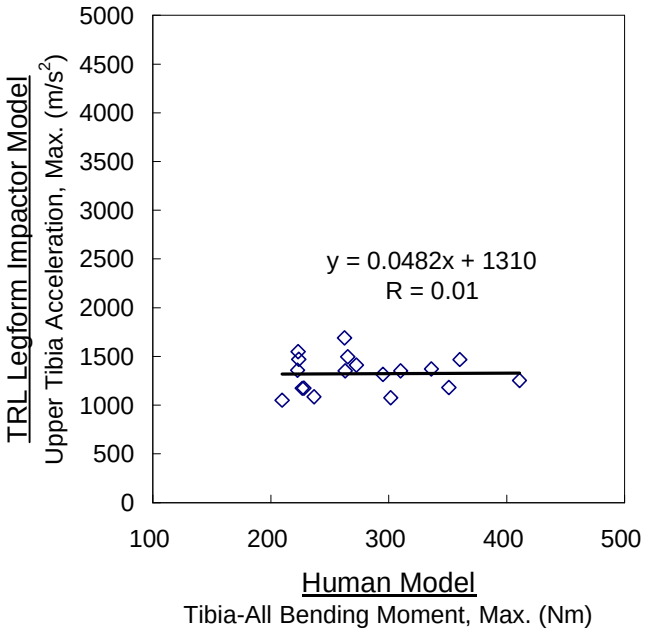

Fig. 13 – Correlation between Upper Tibia Acceleration of TRL legform Impactor Model and Tibia-All Bending Moment of Human Model (Maximum values)

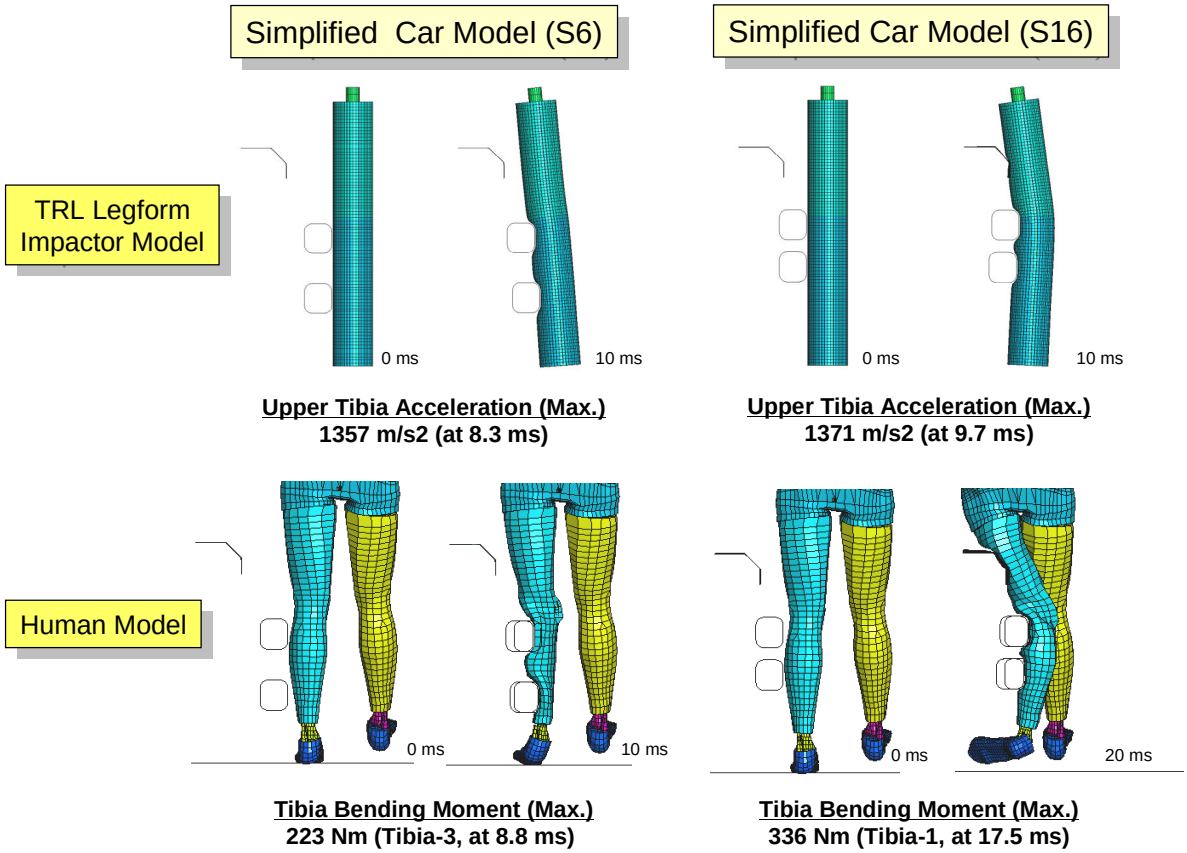

Fig. 14 – Difference of Tibia Bending Moment of Human Model
(Two Different Cars, Similar Upper Tibia Acceleration of TRL Legform Impactor Model)

A2: REANALYSIS OF THE DATA OF THE ACCIDENT RECONSTRUCTION TEST USING THE TRL-LFI

In the second analysis (A2), the correlation between the upper tibia acceleration of the TRL-LFI and tibia fractures sustained by pedestrians involved in car-pedestrian accidents was reanalyzed using the data from the accident reconstruction tests with the TRL-LFI obtained from a past study.

MATERIALS: In the second analysis (A2), test data from Matsui (International Journal of Crashworthiness (IJCrash), 2003) were used. In this paper, the results of 15 accident reconstruction tests using the TRL-LFI are described. Since their original test report (JASIC, 2001) was also available, both of the test data were used in this analysis. The original test report describes 19 test data.

Table 2 shows the test data used as the baseline data of this analysis. The test ID (O1-O19) means the test data obtained from the original test report, and the test ID (IJC1-IJC15) means the test data obtained from Matsui (2003). It is clear from the table that most of the test data were overlapped.

The impact direction of the car to the pedestrian was estimated form a traffic accident analysis report (ITARDA, 2008) and the data files of the original test report.

Table 2: Accident Reconstruction Test Data (all available data combined)

Test ID		Information on the Car-Pedestrian Accidnents								TRL-LFI
				Pedestrian						
Original report	IJCrash	CAR ID	Impact Speed (km/h)	Age (years)	Gender	Stature (cm)	Weight (kg)	Tiba Fracture	Impact direction of Car to Pedestrian	Tibia Upper Accelerations (m/s^2)
O1	-	CAR 1	40	38	Male	175	70	1	Lateral	1091
O2	-	CAR 2	35	64	Female	152	54	1	Back	1101
O3	-	CAR 3	35	61	Female	154	54	1	Lateral	1148
O4	-	CAR 4	35	73	Female	152	60	0	Lateral	1362
O5	IJC1	CAR 5	40	78	Female	unknown	unknown	1	Frontal	1566
O6	IJC2	CAR 6	45	34	Female	160	45	1	Lateral	1534
O7	IJC3	CAR 7	45	90	Male	155	40	1	Lateral	1824
O8	IJC4	CAR 8	40	46	Male	183	65	1	unknown	1763
O9	IJC5	CAR 9	40	72	Female	unknown	unknown	1	Lateral	1613
O10	-	CAR 10	45	46	Male	161	55	0	Lateral	2927
O11	IJC6	CAR 11	45	45	Male	unknown	unknown	1	Lateral	3246
O12	IJC7	CAR 4	45	60	Male	unknown	unknown	1	Lateral	4126
O13	IJC8	CAR 12	40	16	Female	unknown	unknown	0	Lateral	917
O14	IJC9	CAR 4	45	33	Male	160	63	0	Frontal	1602
O15	IJC10	CAR 13	35	59	Male	170	80	0	Lateral	1564
O16	IJC11	CAR 10	40	56	Male	unknown	unknown	0	Lateral	2485
O17	IJC12	CAR 14	40	48	Male	165	58	0	Back	870
O18	IJC13	CAR 15	40	52	Male	159	62	0	Lateral	1109
O19	IJC14	CAR 16	45	78	Male	170	70	0	Oblique	923
-	IJC15	CAR 16	45	78	Male	170	70	0	Oblique	923

Tibia Fracture: (1): Occured, (0): Not occurred

METHODOLOGY: The analysis method employed by Matsui (2003) was reviewed.

Normalization: In Matsui (2003), the upper tibia acceleration data obtained by using the TRL-LFI representing 50th percentile American male (AM50) anthropometry was scaled to the pedestrian involved in the accident reconstructed by using the pedestrian weight; and then an injury risk function was calculated using the scaled data ("Matsui Method"). However, the "Matsui Method" is a completely opposite way compared to the normal injury risk curve development method ("Normal Method") for AM50 size anthropomorphic test device (called as "ATD-AM50" hereafter) as clarified below:

"Normal Method" to develop an injury risk curve for an ATD-AM50

Step 1: Obtain several individual test data by conducting several impact tests using post mortem human subjects

Step 2: Scale the individual test data to the ATD-AM50 anthropometry

Step 3: Develop an injury risk curve for an ATD-AM50 using the scaled test data

"Matsui Method" to develop an injury risk curve for an ATD-AM50

Step 1: Obtain several ATD-AM50 test data by conducting several impact tests using an ATD-AM50

Step 2: Scale the ATD-AM50 test data to the anthropometry of a particular pedestrian

Step 3: Develop an injury risk curve using the scaled test data

Matsui tried to validate tibia fracture probability assessment using an ATD-AM50 with the statistical significance of the injury risk curve obtained from the ATD-AM50 test data scaled to the anthropometry of individual pedestrians involved in accidents reconstructed, which is different from that of AM50.

In the current pedestrian protection regulation, an impactor of AM50 size is used and the pedestrian friendliness of a car is evaluated using the AM50 size test data. This study therefore used the AM50 size test data and evaluated correlation between the test data and the tibia fracture occurrence in the real-world pedestrian accidents.

Data Selection: In Matsui (2003), no data screening was done for the impact direction between the car and pedestrian in the traffic accident. In addition, all the reconstruction tests using the TRL-LFI assumed lateral impact to the leg. Therefore, the impact direction to the leg differed between the accidents and the reconstruction tests when the pedestrian leg was not impacted laterally in the accidents. This could have resulted in different loading patterns of the tibia due to difference in the knee joint stiffness in different loading directions.

In this analysis, therefore, only the accident data for lateral impact to the leg were used for consistency of the impact direction between the accidents and reconstruction tests (see Table 3).

Table 3: Accident Reconstruction Test Data (Data used for this analysis)

Test ID		Information on the Car-Pedestrian Accidnents								TRL-LFI
Original report	IJCrash	CAR ID	Impact Speed (km/h)	Pedestrian					Impact direction of Car to Pedestrian	Upper Tibia Accelerations (m/s^2)
				Age (years)	Gender	Stature (cm)	Weight (kg)	Tiba Fracture		
O1	-	CAR 1	40	38	Male	175	70	1	Lateral	1091
O3	-	CAR 3	35	61	Female	154	54	1	Lateral	1148
O4	-	CAR 4	35	73	Female	152	60	0	Lateral	1362
O6	IJC2	CAR 6	45	34	Female	160	45	1	Lateral	1534
O7	IJC3	CAR 7	45	90	Male	155	40	1	Lateral	1824
O9	IJC5	CAR 9	40	72	Female	unknown	unknown	1	Lateral	1613
O10	-	CAR 10	45	46	Male	161	55	0	Lateral	2927
O11	IJC6	CAR 11	45	45	Male	unknown	unknown	1	Lateral	3246
O12	IJC7	CAR 4	45	60	Male	unknown	unknown	1	Lateral	4126
O13	IJC8	CAR 12	40	16	Female	unknown	unknown	0	Lateral	917
O15	IJC10	CAR 13	35	59	Male	170	80	0	Lateral	1564
O16	IJC11	CAR 10	40	56	Male	unknown	unknown	0	Lateral	2485
O18	IJC13	CAR 15	40	52	Male	159	62	0	Lateral	1109

Tibia Fracture: (1): Occured, (0): Not occurred

RESULTS: Figure 15 shows the injury risk function (dotted line) using the logistic regression and associated p-value obtained in the current study using the data presented in Table 3. The p-value of 0.51 suggests that the tibia upper acceleration of the TRL-LFI is not a good predictor of tibia fracture of a pedestrian occurred in the real-world accidents. In addition, the slope of the injury risk curve is quite shallow, implying a poor injury prediction capability of the upper tibia acceleration of the TRL-LFI.

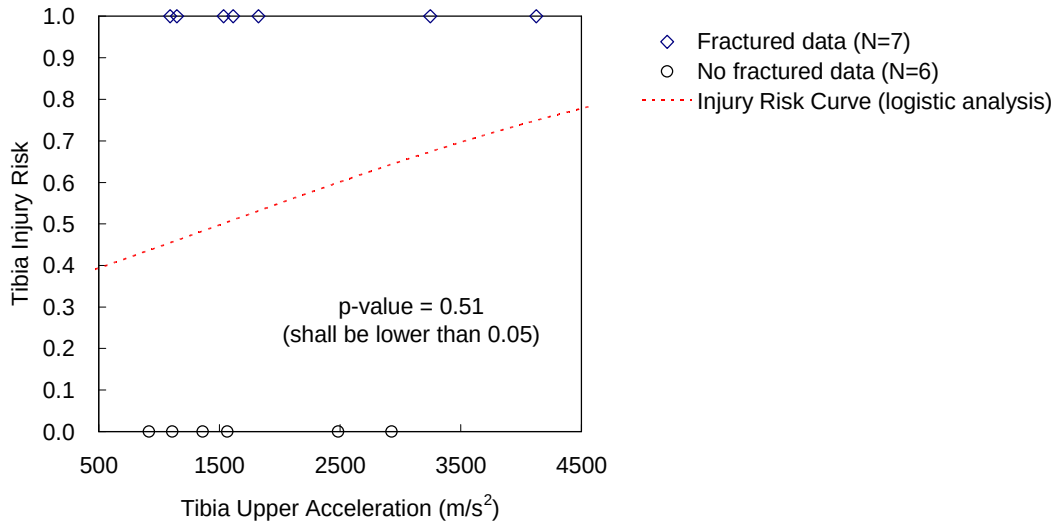

Fig. 15 - Evaluation Results of the Accident Reconstruction Test Data (P-value and Injury Risk Curve)

DISCUSSION

In this study, two different analyses were conducted; A1: analysis on the correlation between the upper tibia acceleration of the TRL-LFI and the tibia bending moment of a human, and A2: reanalysis of the data of the accident reconstruction tests using the TRL-LFI.

From the first analysis (A1), it was found that the correlation between the upper tibia acceleration of the TRL-LFI and the bending moment of the middle third of a human tibia is significantly low (R = 0.01). A possible explanation on this is that although the upper tibia acceleration of the TRL-LFI would well correlate with localized crush type fracture of the tibia due to direct loading, the magnitude of the bending moment of the middle third of the tibia due to inertial loading would be primarily determined by a kinematic constraint provided by a car front geometry. Therefore, it would be difficult to detect the fractures at a wide range of the middle third of the tibia observed in a recent traffic accident study (Otte, 2007) by using the tibia upper acceleration of the TRL-LFI.

From the second analysis (A2), it was found that the upper tibia acceleration of the TRL-LFI poorly correlates with the tibia fractures in real-world pedestrian accidents (p-value = 0.51). The p-value is very different from the one presented by Matsui (2003) (p value = 0.018). The difference mainly came form the difference of the analysis method, especially, 1) the current study used all of the available data in this analysis, 2) the current study only used the cases where the impact direction matched between the car to pedestrian impact direction in the accident and the TRL-LFI to car impact direction in the legform impactor test, and 3) the current study did not scale the results of the legform impactor tests to the anthropometry of individual pedestrians. Although the tibia fracture patterns were not identified in the accident data used in the analysis, it would be presumed that tibia fractures due to

bending of the tibia caused by inertial loading dominate over local crush type tibia fractures due to direct loading to the upper part of the tibia in car-pedestrian accidents from the combination of the results of the first and second analyses. In other words, the poor correlation of the upper tibia acceleration of the TRL-LFI with the tibia fractures in pedestrian accidents would suggest that the tibia fracture due to bending are more frequent than the tibia fracture due to direct loading to the upper part of the tibia.

It is important to note that the reduction of the upper tibia acceleration of the TRL-LFI would provide protection of the tibia for a part of the tibia fracture patterns due to direct loading. In this study, basically, we did not use extremely hard car stiffness because the gtr 9 using the TRL legform impactor was settled in the United Nation in November 2008, and considering the requirements specified in the gtr, the maximum level of the TRL legform impactor acceleration was around 1300 m/s^2 in most of the simulation cases. These cars therefore have a potential for mitigating lower limb injuries associated with a high force applied to the leg, which are not addressed in the current study. However, the upper tibia acceleration of TRL-LFI showed low correlation with the bending moment at the middle third of the tibia which occurred in the real world car-pedestrian accidents as mentioned above. Therefore, in order to conduct more appropriate injury assessment on the tibia of a pedestrian, an impactor which can detect applied bending moment level on the middle third of the tibia, such as the Flexible Pedestrian Legform Impactor (Flex-PLI) developed by Konosu et al. (2009), will be required.

LIMITATIONS

The second analysis (A2) used the AM50 size test data as specified in the current regulation, and validated the correlation between the test data and pedestrian fracture occurred in real-world accidents. The results showed low correlation between them. Theoretically, we can classify the accident data based on the size or gender to create injury risk curves for ATDs representing several different sizes or gender. However, the number of accident data is very limited and it is unrealistic to do this using the currently available accident data. In addition, no discussion on the use of ATDs representing other sizes and/or gender has been raised internationally in the pedestrian regulation at this stage. Therefore, that kind of discussion is premature and would be considered in the future.

CONCLUSIONS

In this study, two different analyses were conducted; A1: analysis of the correlation between the upper tibia acceleration of the TRL-LFI and the bending moment at the middle third of the tibia of a human, and A2: reanalysis of the accident reconstruction test data using the TRL-LFI.

As a result, it was found that the upper tibia acceleration of the TRL-LFI poorly correlated with the bending moment at the middle third of the tibia of a human as well as tibia fractures sustained by pedestrians involved in real-world car-pedestrian accidents. It suggests that bending type tibia fractures dominate in car-pedestrian accidents.

REFERENCES

Bunketorp, O et al.: Experimental Studies on Leg Injuries in Car-Pedestrian Accidents, IRCOBI Conference. pp. 243-255 (1981)

Eppinger, R et al.: Development of Improved Injury Criteria for the Assessment of Advanced Automotive Restraint Systems - II, NHTSA-1999-6407-0005, Section 5.2 (1999)

European Experimental Vehicles Committee (EEVC): EEVC Working Group 10 report: Proposals for methods to evaluate pedestrian protection for passenger cars (1994)

European Enhanced Vehicle-safety Committee (EEVC): EEVC Working Group 17 report: Improved test methods to evaluate pedestrian protection afforded by passenger cars (1998)

Global technical regulation No. 9 (gtr 9): PEDESTRIAN SAFETY (Established in the Global Registry on 12 November 2008), ECE/TRANS/180/Add.9 (2009)

Grosch, L., et al.: Bumper Configurations for Conflicting Rquirements: Existing Performance Versus Pedestrian Protection, 12th ESV Conference. pp. 1266-1273 (1989)

Hayes, W. C., Gerhart, T. N.: Biomechanics of bone: Applications for assessment of bone strength, Bone and Mineral Research, pp. 259-294 (1985)

Institute for Traffic Accident Research and Data Analysis (ITARDA): Traffic Accident Research and Data Analysis Report, ITARDA, pp.360-373 (2008)

Japan Automobile Standards Internationalization Center (JASIC): Research Report for the Pedestrian Safety Test Method (2001)

Kallieris, D., Schmidt, G.: New Aspects of Pedestrian Protection Loading and Injury Pattern in Simulated Pedestrian Accidents, 32nd STAPP Conference, Paper No. 881725 (1988)

Kikuchi, Y., Takahashi, Y., Mori, F. : Development of a Finite Element Model for a Pedestrian Pelvis and Lower Limb, SAE World Congress, paper Number 2006-01-0683 (2006)

Kikuchi, Y., Takahashi, Y., Mori, F. : Full-Scale Validation of a Human FE Model for the Pelvis and Lower Limb of a Pedestrian, SAE World Congress, Paper Number 2008-01-1243 (2008)

Konosu, A., Issiki, T., Tanahashi, M., Suzuki, H.: Development of a Biofidelic Flexible Pedestrian Legform Impactor type GT (Flex-GT), 20th ESV Conference, Paper Number 07-0178 (2007)

Konosu, A., Issiki, T., Takahashi, Y., Suzuki, H., Been, B., Burleigh, M., Hirasawa, T., Kanoshima. H.: Development of A Biofidelic Flexible Pedestrian Legform Impactor Type GTR Prototype - Part 1: Development And Technical Evaluations, 21th ESV Conference, Paper Number 09-0145 (2009)

Matsui, Y.: New injury reference values determined for TRL legform impactor from accident reconstruction test, IJCrash 2003, Vol.8, No.2, pp.179-188 (2003)

Otte, D., Haasper, C.: Characteristics on Tibia and Fibula in Car Impacts to Pedestrians – Influences of Car Bumper Height and Shape, IRCOBI Conference – September 2007, pp. 71-80 (2007)

Takahashi, Y., Kikuchi, Y., Mori, F., Konosu, A.: Advanced FE Lower Limb Model for Pedestrians, 18th ESV Conference, Paper Number 218 (2003)